SEMARAK ILMU PUBLISHING

CFD Letters

Journal homepage:
https://semarakilmu.com.my/journals/index.php/CFD_Letters/index
ISSN: 2180-1363

CFD Analysis on the Development of Pre-Duct Shape to Improve Propeller Performance

Ali Munazid[1], Made Ariana[1,*], I Ketut Aria Pria Utama[2]

[1] Department of Marine Engineering, Institut Teknologi Sepuluh Nopember, Surabaya 60116, Indonesia
[2] Department of Naval Architecture, Institut Teknologi Sepuluh Nopember, Surabaya 60116, Indonesia

ARTICLE INFO

Article history:
Received 9 March 2023
Received in revised form 12 April 2023
Accepted 9 May 2023
Available online 10 December 2023

Keywords:
CFD; Grid Independence; Propeller; Numerical Model; Turbulence Model; Pre-duct

ABSTRACT

Energy saving contributions of Energy Saving Device (ESD) Pre-Duct are reducing energy losses and separation at the stern, increasing the ideal propeller efficiency, increasing the capture of viscous wake that passes through the propeller disk, and increasing the interaction of the propeller and ship hull. The effect of ESD Pre-Duct in front of the propeller on saving of energy is influenced by the accuracy and suitability of the geometry, position, and shape of pre-duct. In this study, the shape of the asymmetric un-circular pre-duct was develop and analysis conducted by compared the effect of the shape of pre-duct on the performance of propeller, the shape of pre-duct: circular (conventional), un-circular, and asymmetric un-circular. Computational Fluid Dynamics (CFD) modelling results using the ANSYS CFX software package with Propeller Open Water (POW) test simulations show that the installation of pre-ducts with several shape developments in general has a significant effect on increasing propeller performance at low propeller rotation speeds, whereas on high propeller rotation even though there is an increase in propeller performance but not significant.

1. Introduction

The ships as a means of sea transportation have transported about 95% of the world's goods are taken from [1]. During 2007, shipping industry is estimated to have emitted 1,046 million tons of CO_2, which corresponds to 3.3% of the global emissions (2.7% international shipping, 0.6% domestic shipping and fishing) are taken from [2]. International shipping in 2011 is estimated to contribute some 3% of the global emissions of CO_2 and the ship propulsion undergone a significant transformation, is dominated by diesel engines as ship propulsion engines with the cost of fuel some 30% of ship operational cost are taken from [3]. The use of engines with fossil fuel that produce NOx, SOx, CO_2, have contributed to increasing environmental pollution and high fuel oil cost. In addition, as the price of fuels hikes, it censes the cost of ship operation.

Against the background of environmental pollution and the use of fuel oil, there are three main factors that make many people and shipping industry question the sustainability and performance of

* *Corresponding author.*
E-mail address: ariana@gmail.com(Made Ariana)

https://doi.org/10.37934/cfdl.16.2.118132

ship propulsion systems, namely rising cost of fuel oil due to rising oil prices, environmental regulations introduced to mitigate of effect of climate change, and the potential introduced of carbon taxes are taken from [3]. Therefore the International Maritime Organization (IMO) issued survey guidelines and certification of the Energy Efficiency Design Index (EEDI) are taken from [4] and guidelines for methods of achieving EEDI are taken from [5]. Rising fuel oil prices and growing pressure to comply with IMO regulations in the marine industry to reduce environmental pollution, there is a demand both new and current ships in operation to develop novel ways or technology to reduce their fuel consumption or improve efficiency energy.

About 85% of the energy used in the ships to overcome the interaction force between the ship hull and the fluid are taken from [3]. The performance of the ship's propulsion system is influenced by fuel oil quality, engine efficiency (conversion of fuel oil into power) and propulsive efficiency (conversion of propeller rotation power into thrust) are taken from [6, 7]. Ship resistance and propeller performance affect: ship speed, ship thrust and fuel oil consumption are taken from [8]. The potential to reductions of power on ships to save energy is reduce ship resistance and increase ship propulsive efficiency are taken from [9, 10] reduce ship resistance, improve efficiency of propulsive, optimization hull/propeller/rudder interaction and optimization ship operation are taken from [7]. Efficiency and saving energy by reducing ship resistance, increasing the performance of the ship's propulsion system and optimal ship operation.

Effort to improving efficiency of propulsors includes choice of design parameters, smooth surface roughness and adaptation to actual hull wake. While optimize hull/propeller/rudder interaction included optimize wake distribution, minimize thrust deduction, upstream low conditioning and recovery of rotational energy are taken from [7]. The sources of energy losses consist of propeller, hull, and shape of the stern. While the basic nature of losses included axial losses, rotational losses, and frictional losses are taken from [11, 12]. As for reducing energy losses caused by axial and rotational phenomena can be done by applying Energy Saving Device (ESD) near the propeller.

The existence of ESD pre-duct in front of the propeller will accelerate the flow through the propeller plan, the increased mass flux through the propeller results in low axial losses are taken from [13]. The contribution of ESD Pre-Duct in saving of energy includes reducing energy losses and separation at the stern of the ship due to flow acceleration effects, increasing ideal propeller efficiency (lower axial kinetic energy losses) due to increased mass flux passing through the propeller, increasing viscous wake capture which passes through the propeller disk, and increases the interaction the hull and propeller are taken from [12, 13] effect pre-duct on fishing vessel are taken from [14], effect geometry of pre-duct are taken from [15]. Thus ESD pre-duct technology is able to increase the performance of propulsors and save energy by reducing the losses that occur in the interaction of hull, propeller and rudder at the stern of the ship.

The effect of ESD pre-duct on energy savings is influenced by the accuracy and suitability of the geometry, position, and shape of pre-duct. The pre-duct shape that have been developed include: conventional pre-duct are taken from [16, 17], eccentric pre-duct are taken from [18-22], asymmetric profile pre-duct are taken from [17], tilting pre-duct are taken from [11], inclined half circular pre-duct are taken from [20, 23-25], un-circular pre-duct are taken from [26, 27]. In general, pre-duct shape is circular and un-circular, which respective shape a different effect on the performance of propulsors and save energy.

Several asymmetric developments at the stern of the ship were reported to be able to increase propeller efficiency and performance, for example asymmetric stern, Daewoo Pre-Swirl System are taken from [28-30], Backer Mewis Duct are taken from [21, 22], Boundary-Layer Alignment Device (BLAD) are taken from [27], Blade Efficiency Improving Stator Duct (BSD) are taken from [25, 31]. Simulation-Based Design Optimization (SBDO) are taken from [26], Crown Duct are taken from [32,

33], etc., with the propeller rotating in one direction resulting in different hydrodynamic characteristics on both sides, which can increase efficiency and save energy.

In the development of circular and un-circular pre-duct shape and several development of asymmetric shapes at the stern of the ship that have been carried out, it is reported that these developments improve propeller performance and propulsors efficiency by reducing energy losses and separation at the stern of the ship, increasing ideal propeller efficiency and viscous wake, and optimizing hull and propeller interaction. Based on this development, a possible pre-duct form was developed by combining un-circular and asymmetrical shape, namely asymmetric un-circular pre-duct form. For this reason, in addition to circular and un-circular pre-duct shape, this paper proposes the development of asymmetrical and un-circular pre-duct shape which expected to increase performance propeller.

Determining and analyzing the performance of the propeller to the shape of the pre-duct is carried out using the Propeller Open Water (POW) simulation and the support of ANSYS CFX Software package analysis. The CFD modeling uses the Reynolds-Averaged Navier Stokes (RANS) equation for three dimensional unsteady viscous incompressible flow, transient blade row methods, the Shear Stress Transport (SST) k-ω turbulence model. Uncertainty analysis of the CFD models with verification validation methodologies and procedures in accordance with procedures and guidelines recommended by International Towing Tank Conference (ITTC) are taken from [34], in addition to comparing the modeling results with the modeling results carried out by institutions and researchers on the same model. Modeling simulation carried out are propellers with and without pre-duct, while the shape of pre-duct are circular, un-circular, and asymmetric un-circular.

2. Methodology

2.1 Computational Fluid Dynamics Model

Studies on the CFD in numerical simulation of propellers, especially propellers of type MP.687 that has been performed. With the development of a numerical viscous flow theoretical approach based on Reynolds-Averaged Navier Stokes (RANS) equations, propeller performance can be determined with good results are taken from [35-38]. The CFD model using ANSYS CFX software package, modeling the flow around the propeller with RANS equation for three dimensional unsteady viscous incompressible flow. The averaged continuity and momentum equation for incompressible flows follow two mass and momentum equations are taken from [39, 40] such as in Eq. (1) and (2).

$$\frac{\partial \rho}{\partial t} + \nabla(\rho \mathrm{U}) = 0 \tag{1}$$

$$\frac{\partial (\rho U)}{\partial t} + \nabla(\rho \mathrm{U} \otimes \mathrm{U}) = -\nabla p + \nabla \mu \left(\nabla U + (\nabla U)^T - \frac{2}{3} \delta \nabla \cdot U \right) + S_M \tag{2}$$

To describe the laminar and turbulent flow of a model, the Navier-Stokes equation can be used, but at a realistic Reynolds numbers the turbulence flow that occurs spans a long turbulence range and large time scale. Therefore, the turbulence model in the CFD model tries to modify, from the original unsteady Navier-Stokes equations to RANS equation. The turbulence model rom RANS equation is also known as the statistical turbulence model, because the turbulence model is to obtained and determine in Eq. (4) using the statistical average procedure. The Reynolds averaged equation given in Eq. (3) and Eq. (4).

$$\frac{\partial \rho}{\partial t} + \frac{\partial}{\partial x_j}\left(\rho U_j\right) = 0 \tag{3}$$

$$\frac{\partial(\rho U)}{\partial t}+\frac{\partial}{\partial x_j}\left(\rho U_i U_J\right)=-\frac{\partial p}{\partial x_j}+\frac{\partial}{\partial x_j}\left(\tau_{ij}-\rho\overline{U_\iota U_J}\right)+S_M \tag{4}$$

Where τ is the molecular stress tensor (including both normal and shear component of the stress)

The SST k-ω is a two-equation eddy-viscosity model. It is a hybrid model combining the Wilcox k-ω and the k-ε models. A blending function, activates the Wilcox model near the wall and the k-ε model in the free stream. The k-ω model is well suited for simulating flow in the viscous sub-layer, and the k-ε model is ideal for predicting flow behavior in regions away from the wall. SST k-ω governing equations in Eq. (5) for turbulence kinetic energy and in Eq. (6) for specific dissipation rate, where *F1* is blending function, v_T is kinematic eddy viscosity.

$$\frac{\partial k}{\partial t}+U_j\frac{\partial k}{\partial x_j}=P_k-\beta^* k\omega+\frac{\partial k}{\partial x_j}\left[(v+\sigma_k v_T)\frac{\partial k}{\partial x_j}\right] \tag{5}$$

$$\frac{\partial \omega}{\partial t}+U_j\frac{\partial \omega}{\partial x_j}=\alpha S^2-\beta\omega^2+\frac{\partial}{\partial x_j}\left[(v+\sigma_\omega v_T)\frac{\partial \omega}{\partial x_j}\right]+2(1-F_1)\sigma_{\omega 2}\frac{1}{\omega}\frac{\partial k}{\partial x_i}\frac{\partial \omega}{\partial x_i} \tag{6}$$

2.2 Geometry

Propeller simulation in open water testing are performed on the existing propeller on the JAPAN Bulk Carrier (JBC) ship, namely the propeller type: MP.687 provided by National Maritime Research Institute (NMRI) are taken from [41]. Propeller geometry as depicted in Figure 1 (a), whereas its particulars are tabulated in

Table 1 while the Pre-duct is an Energy Saving Device (ESD) consisting of a duct and strut which is in front of the propeller, the duct profile is foil NACA 4420 with an angle 20°, as illustrated in Figure 1 (b).

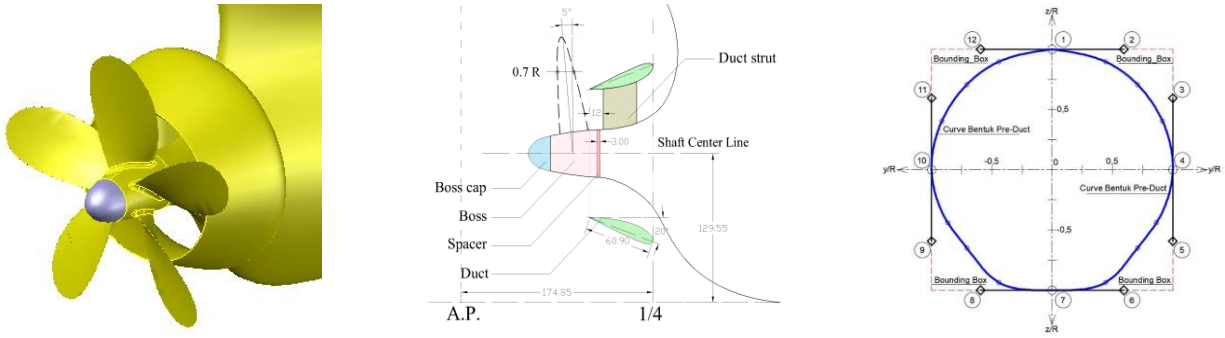

(a) (b) (c)

Fig. 1. (a) View of propeller and pre-duct model, (b) Detail of pre-duct [41], (c) Parametric of pre-duct shape

Table 1
Main particulars of MP 687 propeller model [41]

Parameter		Value	
Number of propeller blades	*Z*	5	-
Diameter propeller	*D*	0.203	m
Boss ratio	D_h/D	0.18	-
Pitch ratio	P_R/D_R	0,75	-
Pitch (constant)	*P*	0,15225	m
Rake angle		5°	-
Expanded area ratio	$A_E/A0$	0,500	-

Using the cubic Bezier Curve method, the accuracy and suitability of the pre-duct shape is determined by twelve points: four fixed end point (1, 4, 7 and 10) and eight control point (2, 3, 5, 6, 8, 9, 11 and 12). The form of the pre-duct curve, the length of control vector is limited by the bounding box, the control point cannot be outside the bounding box and control vector cannot exceed the control vector that is in front of it, as shown in Figure 2 (c). The first Propeller Open Water (POW) simulation condition is a propeller without pre-duct, model code POW-0 as shown Figure 2 (a), the second POW simulation is propeller with circular pre-duct, model code POW-1 as shown in Figure 2 (b). The third POW simulation is propeller with un-circular pre-duct, model code POW2 as shown in Figure 2 (c), while the fourth POW simulation is propeller with asymmetric un-circular pre-duct, model code POW-3 as shown in Figure 2 (d).

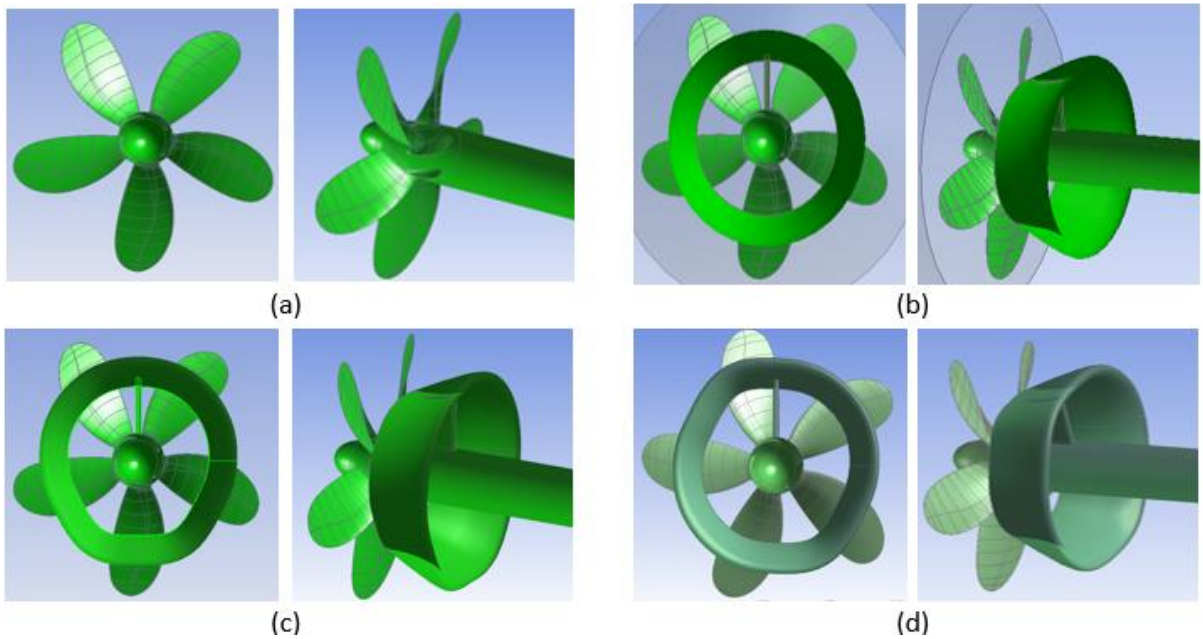

Fig. 2. Various of model (a) POW-0, (b) POW-1, (c) POW-2, (d) POW-3

2.3 Grid Generation

The mesh generation process is carried out using design modeler. The combination of structured and unstructured meshes that are used to discretize the computation domain is referred to as hybrid mesh. Consideration of the intricate geometrical features of the propeller, pre-duct, and shaft, a mash consisting of triangle elements is constructed on surface, and the boundary layer is than refined with prism elements by expanding the surface mesh node. Around the propeller, pre-duct and shaft, the tetrahedral component are inflated to fill this space, while in the distant field, unstructured mesh with modelling is produced to reduce the number of element, as shown in Figure 3.

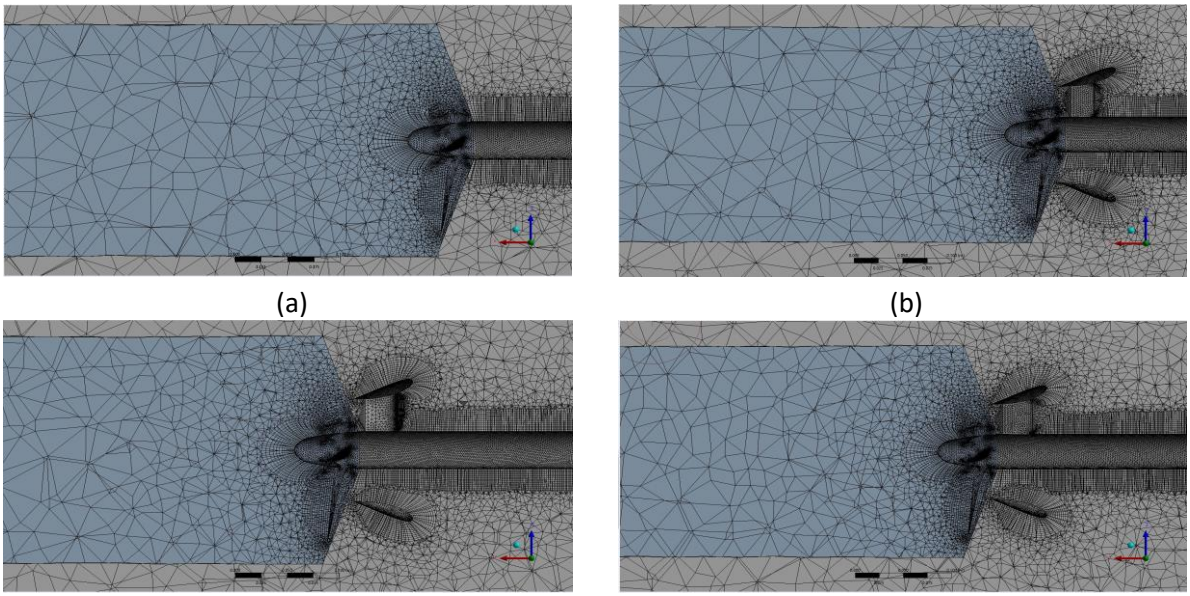

Fig. 3. Various of mesh model (a) POW-0, (b) POW-1, (c) POW-2, (d) POW-3

2.4 Computational Fluid Dynamics Setup

Type of analysis in modeling the MP.687 propeller is transient blade row method by using two cylindrical domains with the following geometries: Stator domain (eight times the length and six times the propeller diameter), and Rotor domain (four times Length and one point two the propeller diameter), as shown Figure 4. On the inlet side, fluid flow conditions are applied with a constant normal speed, on the outlet side, static pressure is applied, while on the propeller, pre-duct and shaft for the finest and coarsest mesh respectively, a no-slip is applied. The flow velocity setting is set at a constant velocity condition, while the propeller rotation speed setting is set at change from 7.3 to 56 rps, which corresponds to advance ratio ranging from J=0.1 to 0.8. To improve the quality of the CFX solution and the efficiency of computer resources and to ensure the convergence and accuracy of the CFD model, solver control is carried out. The solver control settings are defined in Table 2.

Table 2
Solver control settings

Analysis Settings	
Analysis type	Transient blade row
Advection scheme option	High resolution
Transient scheme option	Second order backward Euler
Timestep initialization option	Automatic
Turbulences numeric option	High resolution
Convergence control and criteria	
Fluid timescale control	Coefficient loops
Minimum coefficient loops	1
Maximum coefficient loops	10
Residual type	RMS
Residual target	0,00001

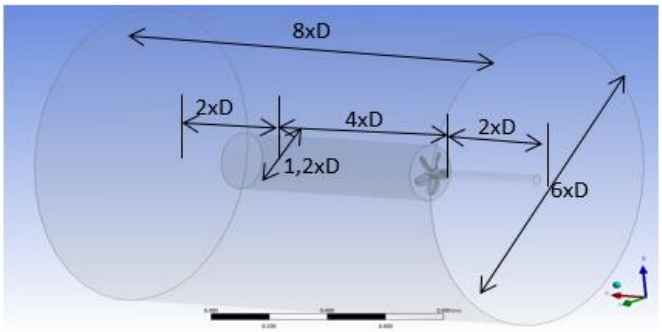

Fig. 4. Computational domain and boundary condition

The solver is based on finite volume method to build a spatial discretization for governing equation to solve the RANS equation for three-dimensional unsteady viscous incompressible flow in global approach, the velocity updates come from the momentum equation and the pressure is extracted from the mass conservation constraints transformed into pressure equation. Closure to the turbulence is achieved by making use of the SST k-ω model for the discretized propeller approach.

In CFD simulation, one of the main sources of simulation uncertainty in predicting fluid flow is the turbulence model, because turbulence model is the most complex phenomenon in classical physics are taken from [42]. Besides that the turbulence model is most important part in CFD which has a very important influence on the stability of the numerical simulation and the accuracy of the calculation results are taken from [43]. According to Boughou *et al.,* [44], Hang *et al.,* [45] explains that the accuracy and resilience of the numerical approaches are essentially need proper industrial turbulence model, in the airfoil and propeller simulation the use of SST K-ω model has good and promising capabilities.

2.5 Grid Independence Study

There are three methods in the grid independent solution to determine the discretization error of CFD modeling, namely: Grid Resolution (GR), General Richardson Extrapolation (GRE) and Grid Convergence Index (GCI) are taken from [43, 46]**.**

2.5.1 Grid Resolution (GR)

The Grid Resolution (GR) method, the most common procedure for determining mesh independent solutions is to gradually increase the mesh size (grid resolution) until there is no significant increase in performance with improvement in mesh size, in other words the optimum mesh size is not significantly affect the quality of the results are taken from [43, 46, 47]. If the difference between the thrust and torque coefficients of the propeller in not more than 2%, then the solution is considered a convergent mesh, see Table 3 and Figure. 5. This is as explained by Suastika are taken from [48] that the difference the two simulation results (Thrust coefficient (K_T) and Torque coefficient ($10K_Q$)) is less than two percent, which assumes that the simulation results are accurate.

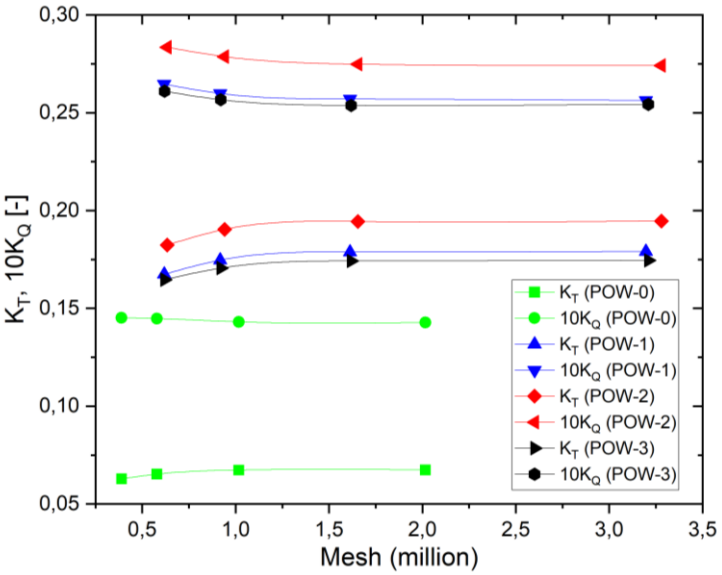

Fig. 5. Grid resolution of propeller

2.5.2 General Richardson Extrapolation (GRE)

The basic principle of the Generalized Richardson Extrapolation (GRE) method in determining or estimating the exact solution of the error expansion series is to use an expansion series that depends on the convergence and refinement rate are taken from [46]. Convergence studies are conducted following a systematic refinement process, a minimum of three solution is required to evaluate the convergence of the model, in addition, grid convergence is based on uncertainty analysis recommendations to the ITTC are taken from [34]. The convergence rate of model is described in the convergence ratio(R_i) can be written as Eq. (7).

$$R_i = \frac{\varepsilon_{i.21}}{\varepsilon_{i.32}} \tag{7}$$

where $\varepsilon_{i.21}$ is different of estimation where is ratio of number of element medium to fine and $\varepsilon_{i.32}$ is different of estimation where is ratio of number of elements fine to coarse.

The convergence of the modelling carried out must be clarified using Eq. (7) to obtain the possible convergence condition. The convergence conditions are possible:

$R_i > 1$	Monotonic divergence
$1 > R_i > 0$	Monotonic convergence
$0 > R_i > -1$	Oscillatory convergence
$R_i < -1$	Oscillatory divergence

For convergence condition, Richarson Extrapolation (RE) is used to estimate the error ($\delta^*_{RE_{i,1}}$) as Eq. (8), and order of accuracy (p_i) as Eq. (9).

$$\delta^*_{RE_{i,1}} = \frac{\varepsilon_{i.21}}{r_i^{p_i}-1} \tag{8}$$

$$p_i = \frac{\ln(\varepsilon_{i.32}/\varepsilon_{i.21})}{\ln(r_i)} \tag{9}$$

Table 3
Grid resolution of ship's propellers

Case	Total number of cell meshing	K_T	$10K_Q$	η	Difference (%)	
					K_T	$10K_Q$
POW-0	389331	0.0629	0.1452	0.5131	6.699	1.714
	578397	0.0653	0.1448	0.5320	3.432	6.202
	1016698	0.0673	0.1431	0.5576	0.109	0.230
	2015604	0.0674	0.1428	0.5595	-	-
POW-1	617523	0.1674	0.2646	0.7496	4.335	1.784
	917402	0.1747	0.2599	0.7963	2.371	1.115
	1612597	0.1788	0.2570	0.8244	0.119	0.263
	3196974	0.1791	0.2563	0.8275	-	-
POW-2	633612	0.1824	0.2835	0.7618	4.406	1.715
	941305	0.1904	0.2787	0.8093	2.759	1.401
	1654613	0.1944	0.2748	0.8382	0.274	0.227
	3280271	0.1947	0.2742	0.8413	-	-
POW-3	619903	0.1647	0.2610	0.7477	3.569	1.622
	920939	0.1706	0.2567	0.7872	1.170	1.170
	1618814	0.1742	0.2537	0.8130	0.192	0.218
	3209299	0.1745	0.2543	0.8128	-	-

2.5.3 Grid Convergence Index (GCI)

The Grid Convergence Index (GCI) method is the method proposed by Roache [49, 50] based on the Richardson Extrapolation method which three meshes to estimate the extrapolated values, this method includes order of accuracy estimation to find extrapolated values are taken from [51]. GCI is a standardized way to report grid convergence quality. It is calculated at refinement steps. Thus, we calculated a GCI for steps from grids 3 to 2, and from 2 to 1.

Due to the complex CFD algorithm, the algorithm is reliable and used with detailed verification and validation. Old methods and often used in ship hydrodynamics in determining discrete uncertainties are the GCI with Factor of Safety (F_S). To calculate the simulation error, grid convergence with a series of similar grids was performed systematically by RE. In the numerical solution, the discretization error ($\delta^*_{RE_{i,1}}$) as Eq. (8), while the FS method of developing ITTC guidelines, which focus on increasing the safety factor as Eq. (10), where F_S = 1.25 is recommended for careful grid studies and F_S = 3 for cases using two grids and accuracy is assumed from theoretical values.

$$U_i = GCI_i = F_S\left|\delta^*_{RE_{i,1}}\right| \tag{10}$$

Based on the results of convergence studies on modeling carried out from POW-0 to POW-3 as shown Table 4. The convergence ratio (R_i) of the model is less than one and more than zero, this means that the model convergence condition is monotonic convergence, according to ITTC in [34] for monotonic convergence condition generalized RE is used to estimate the error ($\delta^*_{RE_{i,1}}$) and uncertainties with factors of safety (U_i) or (GCI_i). The estimated relative error and uncertainties of the model is less than 1.5%, thus the varied convergent mesh has very small errors and uncertainties. So by selecting a small mesh size in a numerical simulation it will provide a better level of precision, for mesh size of POW-0 is 1.0 million, while for POW-1, POW-2 and POW-3 is 1.6 million.

Table 4
The uncertainty analysis of ship's propellers

Outcome		POW-0		POW-1		POW-2		POW-3	
		K_T	$10.K_Q$	K_T	$10.K_Q$	K_T	$10.K_Q$	K_T	$10.K_Q$
Difference of estimation	$\varepsilon_{i.21}$	0.00007	0.00033	0.00021	0.00068	0.00027	0.00062	0.00033	0.00055
	$\varepsilon_{i.32}$	0.00202	0.00174	0.00414	0.00290	0.00405	0.00390	0.00354	0.00300
Refinement ratio	$r_{i.21}$	998906	998906	1584377	1584377	1625658	1625658	1590485	1590485
	$r_{i.32}$	438301	438301	695195	695195	713308	713308	697875	697875
Convergence ratio	R_i	0.03639	0.18904	0.05140	0.23355	0.06699	0.15995	0.09439	0.18416
Order of accuracy	p_i	-0.23985	0.20771	-0.20791	0.19928	-0.18902	0.24841	-0.16529	0.22559
Generalized RE relative error	$\delta^*_{RE_{i.21}}$	0.006%	-0.112%	0.025%	-0.269%	0.041%	-0.171%	-0.070%	-0.174%
	$\delta^*_{RE_{i.32}}$	0.167%	-0.595%	0.485%	-1.152%	0.607%	-1.068%	-0.741%	-0.947%
Grid Convergence Index (GCI)	$GCI_{i.21}$	0.008%	0.141%	0.031%	0.336%	0.031%	0.336%	-0.087%	-0.218%
	$GCI_{i.32}$	0.208%	0.744%	0.607%	1.440%	0.607%	1.440%	-0.927%	-1.183%
Convergence Condition		Monotonic convergence		Monotonic convergence		Monotonic convergence		Monotonic convergence	

3. Results and Discussion

3.1 Validation and Verification of Model

Validation of model is an effort to ensure that the development model represent reality by comparing the results of numerical and experimental modeling. In Figure 6 presents a graph explaining the comparison between experimental results and CFD modeling for open water testing of the MP.687 propeller, experimental results based on experiments conducted by NMRI in [41]. Modeling simulations carried out in open water without pre-duct with constant fluid velocity of 1.179 m/s and propeller rotation from 7.3 to 56 rps which corresponds to advance ratio (*J*) of 0.1 to 0.8. The average error of POW-0 K_T is 4.8%, $10K_Q$ is 8.37%, and open water efficiency (η) is 7.58%. The comparison error E%EFD = (EFD-CFD)/EFDx100, where EFD is Experimental Fluid Dynamic and CFD is Computational Fluid Dynamic.

Verification of model is the process of demonstrating that the model really meets expectations and refers to the appropriate regulation and literature. In addition, verification is carried out on propeller with and without pre-duct to ensure the ability of the model and solver used, verification as described on the grid independent study in 2.5 above. As can be seen from Table 4, the numerical uncertainty in the model (POW-0, POW-1, POW-2 and POW-3) is insignificant.

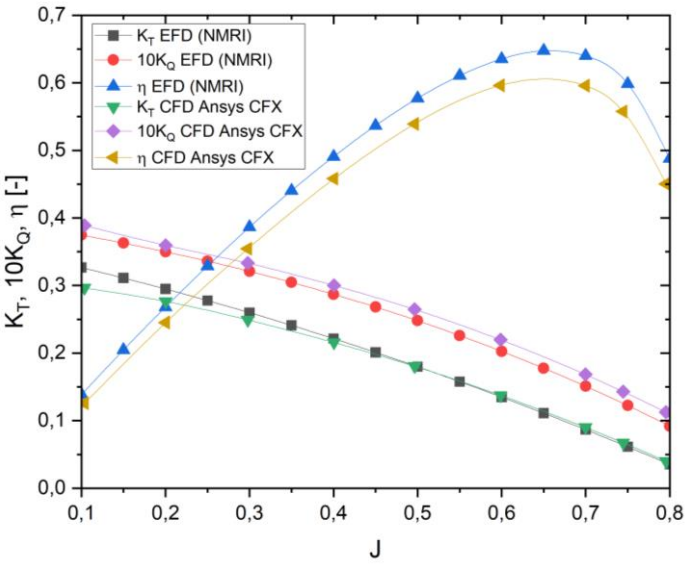

Fig. 6. Propeller performance POW-0

3.2 Effect of Pre-Duct Shape on Propeller Performance

To investigate the effect of the shape of the pre-duct shape on the performance of the propeller, several pre-duct shape were chosen, namely circular, un-circular and asymmetric un-circular shape. With the model that has been verified and validated, modeling of the propeller with and without pre-duct is carried out. In Figure 7, the addition of a pre-duct with a circular, un-circular and asymmetrical shape provides an increase in the value of thrust coefficient (K_T), along with an increase in the thrust coefficient that occurs followed by an increase in the torque coefficient ($10K_Q$). However, the shape of the pre-duct has the effect of increasing efficiency (η), where the increase in efficiency starts at J=0.3 to 0.8.

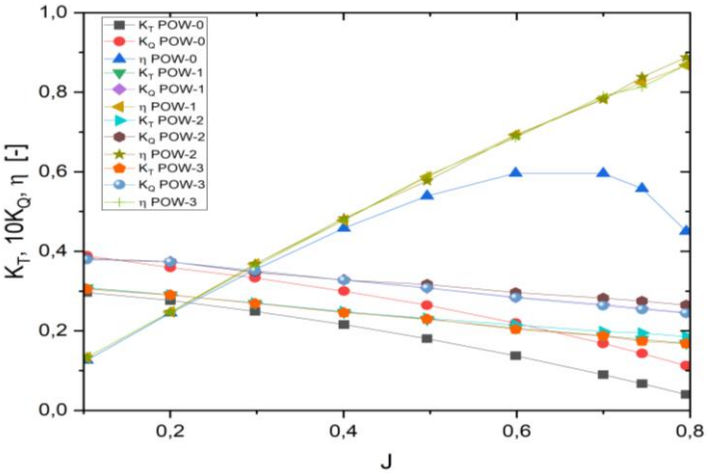

Fig. 7. Comparison of propeller performance POW-0, POW-1, POW-2 and POW-3

The development of the pre-duct shape that has been carried out in front of the propeller has the effect of increasing propeller performance. At low propeller rotation it has a very significant effect on increasing performance, whereas on high propeller rotation even though there is an increase in propeller performance but not significant. In Figure 8, the flow velocity in the simulation without pre-

duct (POW-0) is higher when compared to the simulation with shape of pre-duct (POW-1, POW-2 and POW-3). Due to the placement of the pre-duct in front of the propeller, the velocity of the flow entering the inlet pre-duct has decreased, although it has decreased in the inlet pre-duct, the distribution of fluid flow out of the pre-duct through the outlet pre-duct is more uniform and homogeneous, this which makes positioning the pre-duct with some shape increased efficiency.

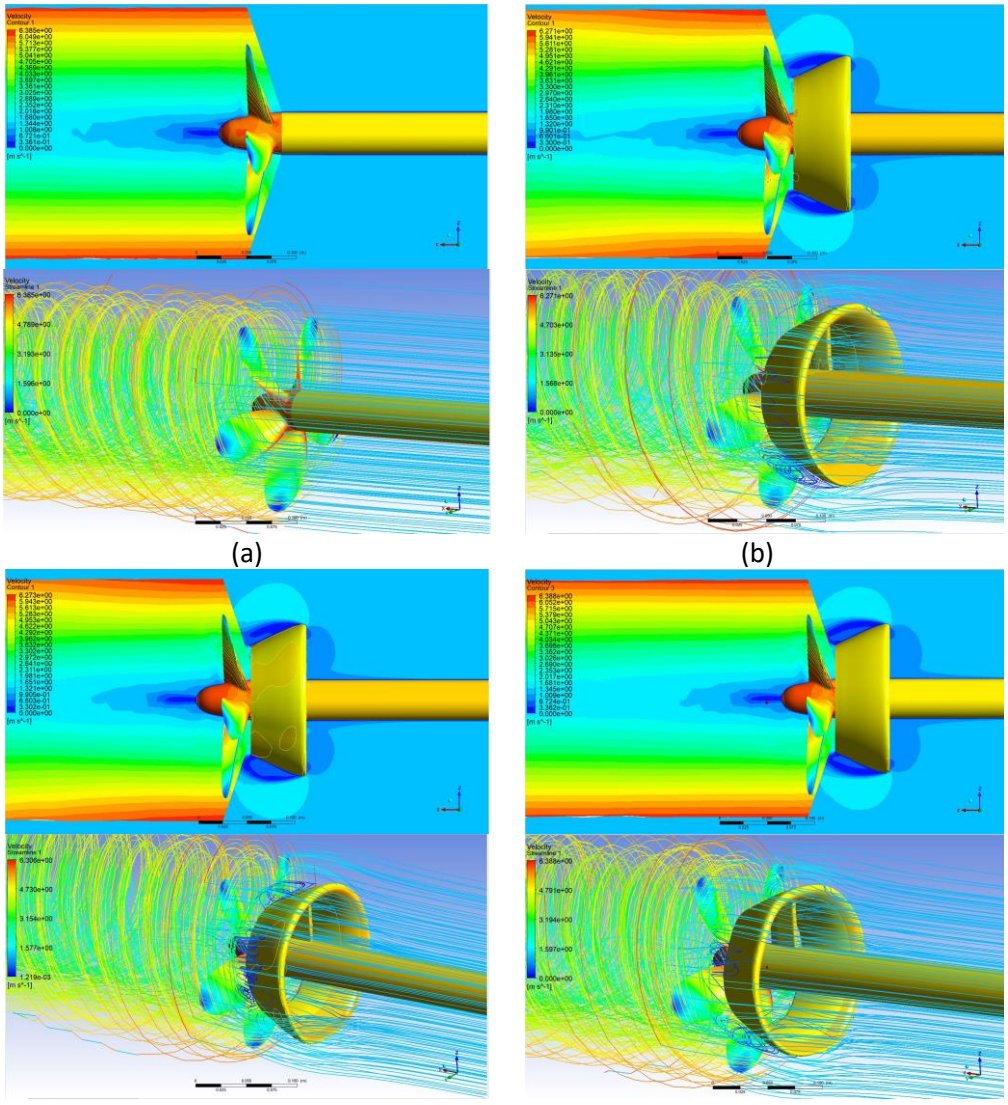

(a) (b) (c) (d)

Fig. 8. Flow velocity (a) POW-0, (b) POW-1, (c) PO-2, and (d) POW-3

The increase in propeller performance, especially the efficiency that occurs in general, is due to the uniformity and homogeneity of the fluid flow in front of the propeller, where the placement of the pre-duct in front of the propeller, even though it reduces the flow velocity, the duct is able to uniform the flow distribution and make the flow more homogeneous before entering the propeller. This phenomenon is consistent according to Ariana *et al.,* [15] pre-duct with variation of duct geometry decreases velocity at the inlet and homogenizes and makes the flow out of the pre-duct homogeneous to the propeller. With a uniform distribution of flow that will pass through the propeller, the trust deduction will be more uniform, causing uniformity in the slipstream and reducing kinetic losses in the slipstream. In addition, the duct will direct the flow in the axial direction to the

propeller, this has a positive influence on uniform loading in a circular direction which will improve propeller performance and increase propeller efficiency.

4. Conclusions

Pre-duct technology with several developments in the shape of the duct placed on the MP.687 propeller generally provides an increase in propeller performance, a significant increase occurs at a value of J = 0.3 to 0.8, this explains that at low propeller rotation it increase performance very large and at high propeller rotation it provides insignificant propeller performance. The increase in performance is due to the increase in thrust and torque from the propeller, because the increase in torque is small and not proportional to the increase in thrust so that the propeller efficiency is very high, especially at low propeller rotation.

The placement of pre-duct with various shapes in front of the propeller reduces in the inflow, even so the distribution of the outflow of the propeller is more uniform and homogeneous, this results in increased propeller thrust and efficiency. The increase in propeller performance, especially the propeller's thrust and efficiency is caused by the uniformity and homogeneity of the fluid entering the propeller, even though the speed entering the propeller decreases, the pre-duct makes the flow that passes through the pre-duct towards the propeller more uniform and homogeneous.

Acknowledgement

The first author, in particular, would like to thank the Design Laboratory of the Department of Naval Architecture at Universitas Hang Tuah for supporting the use of the CFD modelling facility and the Ansys license.

References

[1] Stopford, M. "Engineering change in the merchant fleet." *Address to the Royal Academy of Engineering, London* 10 (2012).

[2] Buhaug, Øyvind, JJ Corbett, Ø. Endresen, V. Eyring, Jasper Faber, Shinichi Hanayama, David S. Lee *et al.*, "Second imo ghg study 2009." (2009).

[3] Carlton, J., J. Aldwinkle, and J. Anderson. "Future ship powering options: exploring alternative methods of ship propulsion." *London: Royal Academy of Engineering* (2013).

[4] IMO, MEPC. "Guide Lines on Survey and Certificaion of the Energy Efficiency Design Index (EEDI)." *MEPC* 63 (2012): 23.

[5] Imo Resolution, M. E. P. C. "Guidelines on the method of Calculation of the Attained Energy Efficiency Design Index (EEDI) for New Ships." *Vasa* 212 (2012): 102-147.

[6] Molland, A. F., S. R. Turnock, and D. A. Hudson. "Ship resistance and propulsion: practical estimation of ship propulsive power." (2011). https://doi.org/10.1017/CBO9780511974113

[7] Molland, A. F., S. R. Turnock, D. A. Hudson, and I. K. A. P. Utama. "Reducing ship emissions: a review of potential practical improvements in the propulsive efficiency of future ships." *International journal of maritime engineering* 156, no. A2 (2014). https://doi.org/10.3940/rina.ijme.2014.a2.289

[8] Kim, Mingyu, and Dong-Woo Park. "A study on the green ship design for ultra large container ship." *해양환경안전학회지* 21, no. 5 (2015): 558-570. https://doi.org/10.7837/kosomes.2015.21.5.558

[9] Molland, A. F., S. R. Turnock, and D. A. Hudson. "Design metrics for evaluating the propulsive efficiency of future ships." (2009): 209-225.

[10] Jadmiko, Edi, Raja Oloan Saut Gurning, Muhammad Badrus Zaman, and Endang Widjiati. "Variations Rake Angle Propeller B–Series Towards Performance and Cavitation with CFD Method." *Journal of Advanced Research in Fluid Mechanics and Thermal Sciences* 106, no. 2 (2023): 78-86. https://doi.org/10.37934/arfmts.106.2.7886

[11] Shin, Hyun-Joon, Jong-Seung Lee, Kang-Hoon Lee, Myung-Ryun Han, Eui-Beom Hur, and Sung-Chul Shin. "Numerical and experimental investigation of conventional and un-conventional preswirl duct for VLCC." *International Journal of Naval Architecture and Ocean Engineering* 5, no. 3 (2013): 414-430. https://doi.org/10.3744/JNAOE.2013.5.3.414

[12] van Terwisga, Tom. "On the working principles of Energy Saving Devices." In *Proceedings of the Third International Symposium on Marine Propulsors. Launceston, Tasmania, Austrailia*. 2013.
[13] Wald, Quentin. "Performance of a propeller in a wake and the interaction of propeller and hull." *Journal of Ship Research* 9, no. 02 (1965): 1-36. https://doi.org/10.5957/jsr.1965.9.2.1
[14] Munazid, A., I. M. Ariana, and I. K. A. P. Utama. "Numerical Study of Pre-Duct on Traditional Fishing Vessels as Energy Saving Device (ESD)." In *IOP Conference Series: Earth and Environmental Science*, vol. 557, no. 1, p. 012049. IOP Publishing, 2020. https://doi.org/10.1088/1755-1315/557/1/012049
[15] Ariana, I. Made, Riyan Bagus Prihandanu, Dhimas Widhi Handani, and A. A. B. Dinariyana. "Investigation of the Effects of the Pre-Duct in a Ship on Propeller–Hull Interactions Using the CFD Method." *CFD Letters* 15, no. 4 (2023): 17-30. https://doi.org/10.37934/cfdl.15.4.1730
[16] Narita, H., H. Yagi, H. D. Johnson, and L. R. Breves. "Development and full-scale experiences of a novel integrated duct propeller." *Trans. SNAME* 89 (1981): 319-346.
[17] T. Kitazawa, M. Hukino, T. Fujimoto, and K. Ueda, "Increase in the propulsive efficiency of a ship with the installation of a nozzle immediately forward of the propeller, Annual Research Report, Hitachi Zosen," 1983.
[18] Sasaki, N., and T. Aono. "Energy saving deviceSLID; Sho energy sochiSLIDno kaihatsu." *Sumitomo Jukikai Giho* 45 (1997).
[19] HSVA The Hamburg Ship Model Basin, "Hydrodynamic Optimization for Life Cycle Performance," 2012.
[20] Gougoulidis, G., and N. Vasileiadis. "An Overview of Hydrodynamic Energy Efficiency Improvement Measures." Athens: The 5th International Symposium On Ship Operations, 2015.
[21] Mewis, Friedrich, and Thomas Guiard. "Mewis duct–new developments, solutions and conclusions." In *Second international symposium on Marine Propulsors*, vol. 18. 2011.
[22] Mewis, Friedrich. "A novel power-saving device for full-form vessels." In *First International Symposium on Marine Propulsors, SMP*, vol. 9. 2009.
[23] INUKAI, Yasuhiko, Masahiro ITABASHI, Yasuhiro SUDO, Takeshi TAKEDA, and Fumitoshi OCHI. "Energy saving device for ship: IHIMU semicircular duct." *IHI engineering review* 40, no. 2 (2007): 59-63.
[24] Inukai, Yasuhiko, Tadaaki Kaneko, Shigeki Nagaya, and Fumitoshi Ochi. "Energy-saving principle of the IHIMU semicircular duct and its application to the flow field around full scale ships." *IHI Engineering Review* 44, no. 1 (2011): 17-22.
[25] Schuiling, Bart, and Tom van Terwisga. "Hydrodynamic working principles of Energy Saving Devices in ship propulsion systems." *International Shipbuilding Progress* 63, no. 3-4 (2017): 255-290. https://doi.org/10.3233/ISP-170134
[26] Furcas, Francesco, Stefano Gaggero, and Diego Villa. "Duct-type ESD: a design application using RANSE-based SBDO."
[27] Tsakalakis, Nikolaos, and Philip Tsichlis. "Guidelines For Energy Efficient Ships." *Final Report for the Targeted Advanced Research for Global Efficiency of Transportation Shipping Program* (2014).
[28] Lee, Jin-Tae, Moon-Chan Kim, Jung-Chun Suh, Soo-Hyung Kim, and Jin-Keun Choi. "Development of a preswirl stator-propeller system for improvement of propulsion efficiency: A symmetric stator propulsion system." *Journal of the Society of Naval Architects of Korea* 29, no. 4 (1992): 132-145.
[29] Lee, Ki-Seung, Moon-Chan Kim, Yong-Jin Shin, and Jin-Gu Kang. "Design of asymmetric pre-swirl stator for KVLCC2 considering angle of attack in non-uniform flow fields of the stern." *Journal of the Society of Naval Architects of Korea* 56, no. 4 (2019): 352-360. https://doi.org/10.3744/SNAK.2019.56.4.352
[30] Khorasanchi, Mahdi, A. H. Day, Osman Turan, Atilla Incecik, and Serkan Turkmen. "What to expect from the hydrodynamic energy saving devices." In *3rd International Conference on Technologies, Operations, Logistics and Modelling for Low Carbon Shipping*. 2013.
[31] Schuiling, Bart. "The design and numerical demonstration of a new energy saving device." In *16th Numerical towing tank symposium*, pp. 141-146. 2013.
[32] Lee, Kwi-Joo, Jung-Sun An, and Han-Joung Kwak. "Comparative Study between Results of Theoretical Calculation and Model Test for Performance Confirmation of "Crown Duct"." *Journal of Ocean Engineering and Technology* 28, no. 1 (2014): 1-5. https://doi.org/10.5574/KSOE.2014.28.1.001
[33] Lee, Kwi-Joo, Jung-Sun An, and Sun-Hee Yang. "A study on the development of energy-saving device "Crown Duct"." *Journal of Ocean Engineering and Technology* 26, no. 5 (2012): 1-4. https://doi.org/10.5574/KSOE.2012.26.5.001
[34] ITTC, "Uncertainty Analysis in CFD Verification and Validation Methodology and Procedures," *ITTC – Recomm. Proced. Guidel.*, p. 12, 2008.
[35] Andersson, J., Hyensjö, M., Eslamdoost, A. and Bensow, R., 2015, September. CFD simulations of the Japan bulk Carrier test case. In *Proceedings of the 18th Numerical Towing Tank Symposium. Cortona, Italy*.
[36] Bekhit, A. S. "Numerical simulation of the ship self-propulsion prediction using body force method and fully

discretized propeller model." In *IOP Conference Series: Materials Science and Engineering*, vol. 400, no. 4, p. 042004. IOP Publishing, 2018. https://doi.org/10.1088/1757-899X/400/4/042004
[37] Bekhit, Adham S., and Adrian Lungu. "Simulation of the POW performance of the JBC propeller." In *AIP Conference Proceedings*, vol. 2116, no. 1. AIP Publishing, 2019. https://doi.org/10.1063/1.5114474
[38] Tu, Tran Ngoc, Do Duc Luu, Nguyen Thi Hai Ha, Nguyen Thi Thu Quynh, and Nguyen Minh Vu. "Numerical prediction of propeller-hull interaction characteristics using RANS method." *Polish Maritime Research* 2 (2019): 163-172. https://doi.org/10.2478/pomr-2019-0036
[39] F. Joel H. and P. Milovan, *Computational Methods for Fluid Dynamics*, Third, Rev. New York, 2002.
[40] Ansys, C. F. X. "ANSYS CFX-solver theory guide." *Ansys CFX Release* 15317 (2009): 724-746.
[41] NMRI, "Tokyo 2015 A Workshop on CFD in Ship Hydrodynamics," 2015. https://t2015.nmri.go.jp/.
[42] Menter, F. R., R. Lechner, and A. Matyushenko. "Best Practice: RANS Turbulence Modeling in Ansys CFD." *ANSYS Inc.: Canonsburg, PA, USA* (2021).
[43] Seeni, Aravind, Parvathy Rajendran, and Hussin Mamat. "A CFD mesh independent solution technique for low Reynolds number propeller." (2021).
[44] Boughou, Smail, Ashraf A. Omar, Omer A. Elsyed, and Mohammed Aldheeb. "Numerical Investigations of Aerodynamic Characteristics Prediction of High-lift Low Reynolds Number Airfoil." *CFD Letters* 14, no. 2 (2022): 111-121. https://doi.org/10.37934/cfdl.14.2.111121
[45] Hang, Leong Chee, Nur Athirah Nadwa Rosli, Mastura Ab Wahid, Norazila Othman, Shabudin Mat, and Mohd Zarhamdy Md Zain. "CFD Analysis on Propeller at Varying Propeller Disc Angle and Advance Ratio." *Journal of Advanced Research in Fluid Mechanics and Thermal Sciences* 96, no. 1 (2022): 82-95. https://doi.org/10.37934/arfmts.96.1.8295
[46] Almohammadi, K. M., D. B. Ingham, L. Ma, and M. Pourkashan. "Computational fluid dynamics (CFD) mesh independency techniques for a straight blade vertical axis wind turbine." *Energy* 58 (2013): 483-493. https://doi.org/10.1016/j.energy.2013.06.012
[47] Kumar, P. Madhan, Paresh Halder, Abdus Samad, and Shin Hyung Rhee. "Wave energy harvesting turbine: Effect of hub-to-tip profile modification." *International Journal of Fluid Machinery and Systems* 11, no. 1 (2018): 55-62. https://doi.org/10.5293/IJFMS.2018.11.1.055
[48] Suastika, Ketut, Gilbert Ebenezer Nadapdap, Muhammad Hafiz Nurwahyu Aliffrananda, Yuda Apri Hermawan, I. Ketut Aria Pria Utama, and Wasis Dwi Aryawan. "Resistance Analysis of a Hydrofoil Supported Watercraft (Hysuwac): A Case Study." *CFD Letters* 14, no. 1 (2022): 87-98. https://doi.org/10.37934/cfdl.14.1.8798
[49] Roache, Patrick J. "Perspective: a method for uniform reporting of grid refinement studies." (1994): 405-413. https://doi.org/10.1115/1.2910291
[50] Roache, Patrick J. "Quantification of uncertainty in computational fluid dynamics." *Annual review of fluid Mechanics* 29, no. 1 (1997): 123-160. https://doi.org/10.1146/annurev.fluid.29.1.123
[51] C. Ismail B., "Procedure for Estimation and Reporting of Discretization Error in CFD Applications," *J. Fluids Eng.*, no. 130, pp. 1–70, 2008. https://doi.org/10.1115/1.2960953